This paper has been accepted for publication in the IEEE Transactions on Vehicular Technologies, 2015.
DOI: not yet available.

Scheduling Policies in Time and Frequency Domains for LTE Downlink Channel: a Performance Comparison

Ole Grøndalen, Andrea Zanella, Kashif Mahmood, Mattia Carpin, Jawad Rasool, Olav N. Østerbø

***Abstract*—A key feature of LTE system is that the packet scheduler can make use of the Channel Quality Information (CQI), which is periodically reported by user equipments either in an aggregate form for the whole downlink channel, or distinguished for each available subchannel. This mechanism allows for wide discretion in resource allocation, thus promoting the flourishing of several scheduling algorithms, with different purposes. It is therefore of great interest to compare the performance of such algorithms in different scenarios. We here carry out a thorough performance analysis of different scheduling algorithms for saturated UDP and TCP traffic sources, and considering both time-domain and frequency-domain versions of the schedulers and for both flat and frequency selective channels. The analysis makes it possible to appreciate the difference among the scheduling algorithms and to assess the performance gain, in terms of cell capacity, users' fairness, and packet service time, obtained by exploiting the richer, but heavier, information carried by subchannel CQI. An important part of this analysis is a throughput guarantee scheduler which we propose in this work. The analysis reveals that the proposed scheduler provides a good tradeoff between cell capacity and fairness both for TCP and UDP traffic sources.**

I. Introduction

Long Term Evolution (LTE), with its IP based flat network architecture, brings higher spectral efficiency and data rate to its users with respect to the previous generations of cellular systems. However, the number of LTE subscriptions in the next future are expected to grow very fast, exceeding 2.6 billion by the end of 2019, with a 10x growth in mobile data traffic between 2013 and 2019 [1].

In order to sustain the increasing demand, an efficient radio resource management module is needed, of which the packet scheduler is an important component. The downlink packet scheduler at the medium access control (MAC) layer is indeed in charge of dynamically allocating the downlink radio resources to the user equipments (UEs), thus determining the order of service and the transmit rate of each user.

One of the key features of LTE is that it allows resource allocation both in the time and the frequency domain. The scheduler can hence decide to allocate all the resources in a given time interval to a single user, or partition them also in the frequency domain, assigning fraction of the available bandwidth to different users in the same time slot. As a result, the scheduler can choose between a simple *Time-Domain* (TD) allocation policy, where a single user gets all the resources in a given time slot, and a more sophisticated *Frequency-Domain* (FD) approach, where resources are allocated with a finer granularity, also exploiting the frequency dimension. The scheduler, furthermore, can make use of the channel quality indication (CQI) that is periodically reported by each UE, either in an aggregate form for the whole downlink channel, or distinguished for each available subchannel. While TD schedulers only need the aggregate CQI, the potential of FD schedulers is fully available when the CQI is provided for each subchannel. The increased flexibility of FD schedulers in resource allocation, however, is paid back in terms of higher complexity and signaling overhead. It is therefore of utmost importance to investigate the scenarios where the FD implementation of the schedulers brings significant improvements over the simpler TD version.

The LTE standard does not impose any restriction on the type of scheduler, thus leaving space for innovation. The main challenge in the design of an LTE scheduler is to find a proper balance between partially contrasting objectives. On the one hand, in fact, resource allocation shall increase the spectral efficiency and, in turn, the cell capacity, which is a key performance index from the operator perspective. On the other hand, resource allocation shall also consider user-related constraints, such as fairness and the Quality of Service (QoS) requirements. This makes the design of the packet scheduler a challenging optimization problem, which has been addressed in different ways [2].

For example, the *Maximum Throughput Scheduler* (MTS), also known as the *opportunistic scheduler*, prioritizes the cell capacity by exploiting channel variations among UEs, while the *Blind Equal Throughput Scheduler* (BETS) aims to provide throughput fairness among the users irrespective of their channel quality, thus at the cost of cell capacity. *Proportional Fair Scheduler* (PFS) somehow balances the opportunistic approach of MTS and the users' fairness objective of BETS by assigning resources based on the average amount of resources assigned to each UE in the past, and its current channel quality. Finally there is also a rich class of schedulers, such as the token bank fair queue (TBFQ) scheduler [3], the Channel-QoS Aware (CQA) schedulers [4], or the Priority Set Scheduler (PSS) [5], which aim at providing some type of QoS guarantees to the

A. Zanella and Matttia Carpin are with the Dept. of Information Engineering, University of Padova, Padova Italy (email: zanella@dei.unipd.it). K. Mahmood, O. Grøndalen and O.N. Østerbøare with Telenor Research, Norway. J. Rasool is with Telenor, Norway.

UEs.

Many of the aforementioned schedulers, along with some others with somewhat similar priority metrics, are already implemented in *ns*-3, which is a widely used network simulator [6]. However, *ns*-3 provides only few LTE schedulers which offer throughput guarantees to users. In this work, we contribute to fill this gap by implementing in *ns*-3 the *Fair Throughput Guarantees Scheduler* (FTGS), which was originally proposed in [7] in TD mode, and that is designed to guarantee equal *long-term* throughput to all UEs, while opportunistically exploiting the temporal variability of the downlink channels to increase the cell capacity. Furthermore, here we extend FTGS to work in FD mode.

We then compare the two versions of the FTGS algorithm with other representative schedulers for LTE systems, already supported by *ns*-3, namely MTS, BETS, PFS, CQA and PSS, both for flat and frequency selective fading channels. We observe that the first three schedulers, MTS, BETS, and PFS, are quite popular and commonly considered in many studies, being representative of alternative philosophies in resource management, as it will be explained later. Furthermore, they come in two versions, either pure TD or pure FD. For this reason, they will be collectively referred to as "pure algorithms" in the following. Conversely, CQA and PSS are more recent algorithms that adopt a hybrid TD/FD approach, for which reason they are here referred to as "hybrid algorithms".

The analysis reveals that FTGS provides a good trade-off between cell capacity and fairness in different scenarios, both for UDP and TCP traffic sources. Furthermore, we observe that the FD version of FTGS can bring substantial improvements over TD in frequency selective channels, when the channel dispersion is large, thereby justifying the increased complexity of FD implementation. In addition, we analyze the inter-scheduling time at MAC layer of FTGS, BETS, and PFS, in both fast and slow fading scenarios, in order to assess the potential impact of such scheduling algorithms on delay-sensitive applications. The analysis shows that the inter-scheduling time of the TD version of FTGS can be indeed critical in the presence of slow fading channels. However, the FD version of FTGS can dramatically reduce the inter-scheduling time and the service time of high-layer packets in case of frequency selective channels, thus alleviating the aforementioned problem.

In summary, the main contributions of this paper are the following:[1]

- We propose an extension of the FTGS scheduler for the FD mode that makes it possible a finer distribution of the transmission resources to the UEs, thus potentially improving the spectral efficiency. As ancillary contribution, we enrich the existing *ns*-3 repository with schedulers that support long term fairness and throughput guarantees to the UEs.[2]
- We investigate and compare the performance of different schedulers for LTE downlink channel. The scheduling algorithms have been chosen as representative of different resource-management policies, ranging from purely opportunistic to perfectly fair approaches.
- The performance analysis is carried our for different types of fading channels (slow/fast and flat/frequency selective fading), and both for the TD and FD versions of the schedulers, when possible. In this way, the comparison gives insights on the advantages of the frequency agility offered by the FD versions of the schedulers in different channel conditions.
- We considered both UDP and TCP traffic sources. Furthermore, service time statistics are also analyzed and compared for different schedulers, when varying the fading characteristics.
- We analyze the opportunistic gain of the FTGS, with BETS being the benchmark, for the case when the users signal to interference noise ratios are disparate.
- Finally, the robustness of the FTGS scheduler is tested against the impact of an imprecise channel estimation.

The remainder of this paper is organized as follows. Sec. II briefly summarizes the related work. We describe the system model, simulation scenario and performance metric in Sec. III. Sec. IV focuses on various scheduling policies considered in this paper. Sec. V describes the simulation setup, while Sec. VI shows the numerical results. Finally, conclusions and future works are presented in Sec. VII.

II. Related work

The performance analysis of downlink scheduling can be carried out either at the MAC layer or at the transport layer where, in the latter, the effect on transmission control protocol (TCP) is of high importance. While the MAC throughput analysis has its own benefits, a huge fraction of today's data is carried via HTTP [8] which uses TCP because it is reliable, well understood, and can be conveniently managed by firewalls and security systems. However, it is not always straightforward to infer TCP throughput from MAC performance for a given scheduling algorithm. It is therefore essential to investigate the performance of the scheduling algorithms when they handle TCP traffic as well.

Acknowledging this need, the performance analysis presented in [9], which compared the MAC-layer throughput of some schedulers available in *ns*-3, has been extended in [10] to TCP traffic sources, comparing both the aggregate and per-user TCP throughput achieved by the different schedulers. In [11] a TCP-aware scheduling algorithm, named Queue MW, has been implemented in *ns*-3. The performance of Queue MW is then compared against other scheduling policies in terms of throughput and delay for different queue sizes at the evolved node B (eNodeB). Similarly the adverse effect, due to the variability in inter-scheduling time brought by PFS on TCP and its congestion control mechanism is highlighted in [12]. It needs to be mentioned that PFS is commonly used as a reference scheduler for many performance analysis study. For example the fairness and bit rate characteristics of MTS and

[1] A preliminary version of this work has been accepted in ICC 2015. As for IEEE policy, this manuscript extends the conference version with about 30% of new material, including additional results and deeper discussion and analysis of the schedulers performance.

[2] The software can be downloaded from http://goo.gl/3BYxOC.

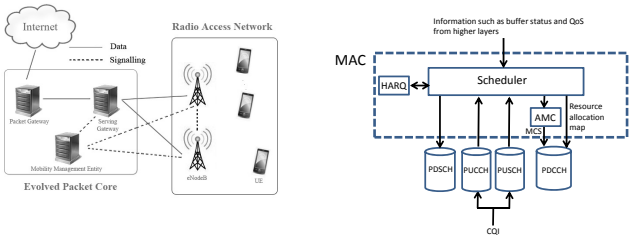

(a) (b)

Fig. 1. (a) LTE high level architecture and (b) interaction of entities relevant for downlink MAC scheduling.

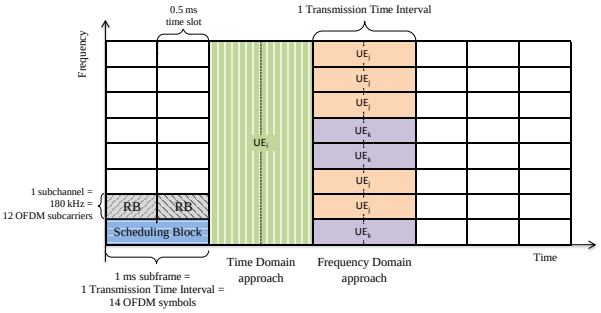

Fig. 2. LTE frame structure.

PFS are compared in [13]. A PFS based scheduling algorithm is proposed in [14] which takes into account the frequency diversity and the multi-user diversity gain simultaneously. The algorithm is tested by simulating a heterogeneous environment consisting of both high-mobility and low mobility users, with saturated sources. The MAC analysis reveals substantial improvements in the overall cell throughput as compared to raw PFS. Finally the effect of the chosen scheduling algorithm on cell spectral efficiency and packet delay experienced by the user for VoIP and video traffic is analyzed in [15].

In a nutshell, there has been a growing interest in the design and performance comparison of scheduling algorithms for LTE taking into account both UDP and TCP traffic. However, to the best of the authors knowledge, a comparison with opportunistic, but users' fair schedulers, capable of providing throughput guarantees to users while exploiting the specific resource allocation structure of LTE, has not yet been carried out. This paper is a first contribution to fill such a gap.

III. System Model

In this section we first recall the reference architecture of the LTE system, which is necessary to understand the working principle of the packet scheduler. Then, we describe the framework considered in our work.

A. LTE basics

The high-level architecture of the LTE system is sketched in Fig. 1(a). There are two keys components: the radio access network (RAN) and the evolved packet core (EPC). The RAN provides the wireless connectivity between the eNodeB and the UE while the EPC is responsible, among other things, for connecting the RAN to the Internet for end-to-end communication. The resource allocation in LTE is done in a centralized manner and, as such, both the uplink and the downlink schedulers reside inside the eNodeB.

MAC scheduler shown in Fig. 1(b) is one of the key components of layer 2 radio protocol stack in eNB. Physical downlink shared channel (PDSCH) is used to transmit the downlink data from eNB. The scheduling decision is based amongst others on the CQI reported by the UE which is carried either by the physical uplink control channel (PUCCH) or physical uplink shared channel (PUSCH) [16]. The adaptive modulation and coding (AMC) block selects the proper modulation and coding scheme (MCS) to maximize the supported throughput for a given target block error rate. The chosen MCS and resource allocation map are sent on the physical downlink control channel (PDCCH). It is important to mention here the HARQ retransmission mechanism at the MAC layer which is performed through the exchange of ACK/NACK between eNB and UE.

While the uplink channel of LTE is based on a Single Carrier Frequency Division Multiple Access (SC-FDMA) scheme [16], the downlink channel, which is the focus of this paper, makes use of Orthogonal Frequency Division Multiple Access (OFDMA).

The frame structure of the downlink air interface is shown in Fig. 2. A frame consists of 10 sub-frames where the length of each sub-frame is 1 ms, which is also the Transmission Time Interval (TTI). Each sub-frame is further divided into two slots of 0.5 ms each. A slot consists of 7 OFDM symbols in the time domain (normal cyclic prefix), and is divided in the frequency domain into sub-channels of 180 KHz each. A time/frequency radio resource spanning over one sub-channel in the FD and over one time-slot in the TD is called a Resource Block (RB).

A Resource Block Group (RBG) consists of multiple adjacent RBs in a single time slot. In each 1 ms subframe, the MAC scheduler is responsible for allocating the RBGs to one or more UEs according to the specific scheduling metric, and the TD or FD approach. The bit rate and capacity of each RB are determined by the MCS used in that RB. The LTE standard imposes a restriction in that all the RB's of an RGB assigned to a user must use the same MCS.

In this work we consider non-persistent scheduling, where the resource allocation is repeated at each subframe as opposed to the semi-persistent scheduling for which the resource allocation remains valid for multiple subframes.

Resource Allocation Type specifies the way in which the scheduler allocates RBs for each transmission. The actual version of *ns*-3 supports only Allocation Type 0, where first the scheduler divides RBs in RBG, with a number of RBs in each group that depends on the system bandwidth. Then, each RBG is assigned to a UE according to the scheduling metric. For example, if we consider an overall cell bandwidth of 25 RBs, each RBG contains 2 RBs [16], thus the scheduler must assign for each time slot the 12 available RBGs to a user according to the scheduling metric, leaving the last RB

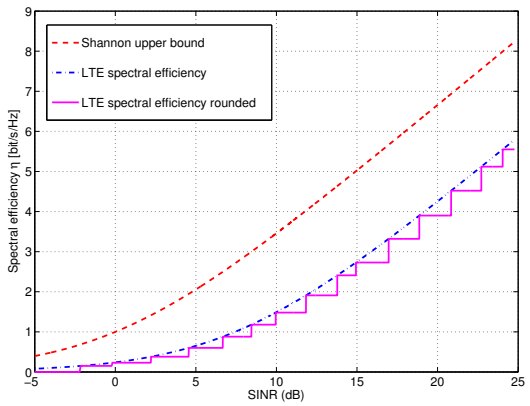

Fig. 3. Spectral efficiencies as a function of the SINR.

unscheduled.

When performing the scheduling decision, the MAC scheduler can make use of the CQI reported by each UE and used by the radio resource management to estimate the channel's quality of that UE [16]. There are two possible channel quality estimations that each UE can perform: the *wideband*estimation, where a single CQI value is reported for the entire bandwidth, and the *subband* estimation, where the CQI is evaluated and reported for each RB.

We assume that the TD scheduling approach makes use of the wideband CQI, while the FD implementation requires the subband CQI, unless otherwise specified.

B. Spectral efficiency

Denoting by γ the SINR of a UE, its spectral efficiency can be expressed as

$$\eta = \log_2\left(1 + \frac{\gamma}{\Gamma}\right), \tag{1}$$

where Γ, sometimes referred to as $\mathrm{SNR}_{\mathrm{gap}}$ [17], accounts for the difference between the theoretical Shannon bound and the efficiency obtained by practical modulation schemes, and for a given target bit error rate (BER) can be expressed as $\Gamma = -\ln\left(5 \cdot BER\right)/1.5$ [18].

The spectral efficiency is then mapped to the CQI according to Tab. I, where η_{th} defines the upper boundary of the interval of η values associated to the same CQI. We assume that each UE reports this CQI value to the eNodeB before the scheduling decision takes place [19]. It should be noted that a higher CQI value corresponds to a better channel.

TABLE I
SPECTRAL EFFICIENCY AND CQI MAPPING.

CQI	0	1	2	3	4	5	6	7
η_{th}	0.15	0.23	0.38	0.6	0.88	1.18	1.48	1.91
CQI	8	9	10	11	12	13	14	15
η_{th}	2.41	2.73	3.32	3.9	4.52	5.12	5.55	>5.55

Fig. 3 shows the difference between the spectral efficiencies computed using Shannon upper bound ($\Gamma = 1$) and that given by (1) for a target $\mathrm{BER} = 5 \cdot 10^{-5}$ ($\Gamma \simeq 5.53$). We also plot the discrete version of the spectral efficiency, obtained from Tab. I. The *ns*-3 implementation of the LTE network makes use of this version according to the standard specifications [19].

C. Simulation scenario

We consider a system in which a single eNodeB serves a population of N static backlogged users. Further we assume that the eNodeB is capable of estimating the statistical distribution of the SINR of each UE that, in turn, provides its current wideband or subband CQI at each TTI, depending on whether TD or FD schedulers are considered. The impact of imperfect channel estimation on FTGS will also be analyzed in Sec. VI-D.

Within a single cell, LTE networks provide orthogonality among users, both in the downlink and uplink. This means that different users, served by the same eNodeB, are assigned different resources in order to avoid interference among them. In this work, since we assume a single eNodeB and a single cell, we are implicitly neglecting the presence of interference. However, since the analysis and the scheduling algorithm can still be applied in the presence of interference, we use the term SINR even for the single cell scenario.

Finally, we consider a path loss channel model affected by either flat or frequency selective fading, and by additive white Gaussian noise.

D. Performance Indexes

The purpose of this study is to compare the different scheduling policies for the downlink channel of an LTE system, when varying the channel conditions and the number of users. As mentioned, each scheduling algorithm offers a different balance between the overall spectral efficiency of the cell, and the service offered to each user. Therefore, the performance comparison will be performed considering a set of indexes, both at the MAC and transport layer. More specifically, we will analyze the *cell throughput*, defined as the aggregate throughput obtained by all the UEs in the cell, together with the Jain's fairness index J, defined as [20]

$$J = \frac{\left(\sum_{i=1}^{N} x_i\right)^2}{N \sum_{i=1}^{N} x_i^2}. \tag{2}$$

where x_i is the throughput achieved by the ith UE. It should be noted that $J = 1/N$ corresponds to the minimum fairness, while $J = 1$ indicates perfect fairness among the users in the system. In addition, we consider the statistical distribution of the inter-scheduling time, that is the time a UE is not scheduled for transmission. From this metric, we then estimate the mean and standard deviation of higher-layer packet service time, which is relevant for delay-sensitive applications.

IV. SCHEDULING POLICIES

In this section we describe the scheduling policies considered in our analysis. The chosen schedulers are representative of different philosophies in resource management, ranging from the maximization of the cell spectral efficiency with no concern of users fairness, to the maximization of users fairness with no concern on cell spectral efficiency. We start by

describing the TD version of the schedulers, where all RBGs are allocated to a single UE at each subframe. Successively, we extend the analysis to the FD case, where RBGs in the same subframe can be allocated to different UEs. Finally, we describe two schedulers that combine FD and TD approaches.

A. TD version of the schedulers

The scheduling decision in the time domain dictates which UE will get all the RBGs in the upcoming subframe k. The decision is based on a priority metric that varies for the different scheduling algorithms. In the following, we describe the metric of the schedulers considered in this study.

1) Maximum Throughput Scheduler (MTS): As discussed earlier, opportunistic schedulers exploit instantaneous channel variations to maximize the cell throughput. One such algorithm is MTS that schedules the users with more favorable channel conditions. The associated scheduling metric is then

$$i_{_{MTS}}(k) = \arg\max_{1\leq i\leq N} r_i(k), \tag{3}$$

where $r_i(k)$ is the instantaneous rate that can be achieved by user i when assigned the RBGs in the kth subframe, and it depends on the wideband CQI reported by the user. It is worth remarking that MTS can achieve the maximum cell throughput but, if the average SINR distributions of different users are extremely unbalanced, it could result in the starvation of UEs experiencing bad channel conditions.

2) Blind Equal Throughput Scheduler (BETS): As opposed to MTS, the objective of BETS is to guarantee equal average throughput to all users in the system. Accordingly, the scheduling metric for BETS is defined as follows [2]

$$i_{_{BETS}}(k) = \arg\max_{1\leq i\leq N} \frac{1}{\zeta_i(k)}, \tag{4}$$

where $\zeta_i(k)$ is the average throughput of the i-th UE up to subframe k, which is updated as (see [16])

$$\zeta_i(k+1) = \beta\cdot\zeta_i(k) + (1-\beta)\cdot r_i(k), \tag{5}$$

where $\beta \in [0,1]$. It should be noted that BETS is a channel-unaware scheduler, and thus it is not very efficient in terms of cell throughput. Due to its simplicity, the long-term throughput achieved by BETS can actually be computed in a closed form, as explained in Appendix A-III.

3) Proportional Fair Scheduler (PFS): PFS tries to find a balance between the opportunistic approach of MTS and the fairness attitude of BETS by adjusting the scheduling index used by BETS according to the current channel gain, as for MTS. The PFS scheduling metric is hence given by:

$$i_{_{PFS}}(k) = \arg\max_{1\leq i\leq N} \frac{r_i(k)}{\zeta_i(k)}. \tag{6}$$

4) Fair Throughput Guarantees Scheduler (FTGS): In the literature, many priority based opportunistic schedulers have been proposed, where different priorities are given to UEs based on certain fairness criteria. FTGS is one such scheduler, which was originally proposed in [7] in the TD version. The scheduling metric of the FTGS is given as

$$i_{_{FTGS}}(k) = \arg\max_{1\leq i\leq N} \frac{r_i(k)}{\alpha_i}, \tag{7}$$

where α_i is a weighting factor assigned to user i in order to maximize the throughput guarantees to all UEs in the long term. These weighting factors depend on the SINR distributions of the users, such that a user with poor average channel conditions, i.e., lower average SINR, is given higher priority compared to users with better average channel conditions. It should be noted that, when all the users have equal average SINR distributions, we have $\alpha_i = \alpha\ \forall i$ and the FTGS reduces to the purely opportunistic MTS.

The factors $\{\alpha_i\}$ in (7) are obtained as explained in Appendix A-I, where the method proposed in [7] is slightly adjusted to account for the practical aspects of LTE system related to resource allocation. Note that the coefficients α_i have to be computed any time the average SINR experienced by the different users changes. In a real-life wireless network, the average SINR normally changes on a time-scale of several seconds, while the throughput guarantees are calculated over time-windows of less than one hundred milliseconds (see, e.g., [21]). Therefore, we assume the average SINR can be considered constant in the time-window over which the throughput guarantees are calculated.

B. FD generalization of the schedulers

So far, we have assumed that all the RBGs in a subframe have to be assigned to a single UE. We here consider the possibility of scheduling multiple UEs in the same time slot by assigning one single RBG at a time.

We then denote by $r_i(k,\ell)$ the rate that user i can get from RBG ℓ at slot k, and define the scheduling index for the FD version of MTS as follows:

$$\hat{i}_{_{MTS}}(k,\ell) = \arg\max_{1\leq i\leq N} r_i(k,\ell)\,. \tag{8}$$

The FD version of BETS is based on the same principle of the TD version, that is providing equal throughput to all UEs. The only difference is that RBGs are allocated one at a time, and the throughput of the interested UE is updated after each allocation.

The FD version of PFS is, again, the result of the combination of MTS and BETS approaches, so that the scheduling index of UE i in RBG ℓ at subframe k is defined as

$$\hat{i}_{_{PFS}}(k,\ell) = \arg\max_{1\leq i\leq N} \frac{r_i(k,\ell)}{\hat{\zeta}_i(k,\ell)}\,, \tag{9}$$

where $\hat{\zeta}_i(k,\ell)$ is the throughput of user i at the allocation time of the ℓth RBGs in the kth subframe.

For what concerns FTGS, we observe that the rationale to derive the coefficients $\{\alpha_i\}$ presented in Appendix A-I can be extended to the frequency domain. This is of particular interest when a frequency selective channel is considered. In this context, making use of the subband CQI, the eNodeB can guarantee more fair scheduling while improving the cell throughput. If we take the channel to be frequency selective, with each subband assumed to be narrow enough to be considered frequency-flat, the SINR is still exponentially distributed, and the α_i values computed for the TD case and reported in Tab. V are still valid and can be reused. Otherwise, the optimization problem needs to be solved again using the actual

SINR distribution, and a new set of α_i's can be obtained. The FTGS scheduling metric for the FD approach then becomes

$$\hat{i}_{FTGS}(k,l) = \arg\max_{1\le i\le N} \frac{r_i(k,l)}{\alpha_i}\,. \tag{10}$$

The FD implementation achieves higher granularity at the cost of higher implementation complexity. It is, therefore, important to investigate the trade-off between system improvement due to FD approach and increased computational complexity and signaling cost. This complexity not only comes from the scheduler, in the eNodeB, that needs to provide flexible allocation in the frequency domain, but also from the UE, that needs to measure the CQIs for each subband, instead of reporting a single value for the entire bandwidth.

We argue that the improvements brought by the FD implementation depend on the frequency selectivity of the channel, that is, the channel dispersion. A parameter that is normally used to define the channel dispersion is the root-mean square (rms) delay spread, τ_{rms}, which corresponds to the second-order central moment of the channel impulse response [22], that is

$$\tau_{\mathrm{rms}} = \sqrt{\left(\bar{\tau}^2\right) - \left(\bar{\tau}\right)^2}, \tag{11}$$

with

$$\bar{\tau}^n = \frac{\sum_{i=1}^{\mathcal{P}} \mathbf{E}\left[|g_i|^2\right] \tau_i^n}{\sum_{i=1}^{\mathcal{P}} \mathbf{E}\left[|g_i|^2\right]}, \tag{12}$$

where $\mathcal{P}$ is the number of signal replicas generated by multipath propagation and received with non-negligible power, τ_i is the delay of the i-th path, and $\mathbf{E}\left[|g_i|^2\right]$ is the average power gain of the i-th path, with $\mathbf{E}\left[.\right]$ denoting the statistical expectation.

C. Joint TD-FD schedulers

Besides these pure TD/FD algorithms, we also consider some schedulers that adopt a hybrid TD-FD approach. These schedulers operate in two stages: first a set of users to be served in the next subframe are selected, then the RBGs of the subframes are allocated to such users based on a FD scheduling algorithm. For our analysis in this paper, we consider the following two schedulers.

1) Priority Set Scheduler (PSS): The first stage of PSS [5] consists of extracting N_{max} users to be served in the second stage, according with an FD approach. For each subframe k, PSS first divides the users in two groups, based on whether their average throughput $\zeta_i(k)$ is lower (group 1) or higher (group 2) than the target bit rate. UEs in group 1 have priority over those in group 2. Users in group one are then sorted according to a priority metric based only on the average user throughput, as for BETS, while users in the second group are sorted according to another priority metric that, besides the average throughput, also accounts for the estimated wideband throughput of the users, as for PFS. The N_{max} users with top priority are selected for the second stage. Then, the generic ℓth RBGs in the subframe is assigned to the UE with maximum Proportional Fair Scheduled (FD-PFsch) metric, i.e.,

$$\hat{i}_{PSS}(k,\ell) = \arg\max_{1\le i\le N} \frac{r_i(k,\ell)}{\zeta_{sch,i}(k)}\,, \tag{13}$$

where $\zeta_{sch,i}(k)$ is similar to the past average throughput for UE i, but in contrast to $\zeta_i(k)$ it is updated only when the UE is actually scheduled, e.g. when the rate given to UE i is actually larger than zero.

2) Channel and QoS Aware scheduler (CQA): In each subframe k, the CQA scheduler [4] first groups the users according to the index

$$i_{td}(k) = \left\lceil \frac{d_i(k)}{g} \right\rceil, \tag{14}$$

where $d_i(k)$ is the head-of-line packet delay of user i in subframe k, and g is a constant. These groups are served in decreasing order of $i_{td}(k)$. The UEs in each group, in turn, are assigned the RBGs in that subframe. To this end, for each RBG, the UEs are ordered according to a second metric, defined as

$$\hat{i}_{fd,CQA}(k,\ell) = d_i(k)\,\frac{GBR_i}{\zeta_i(k)}\,i_{ca}(k,\ell)\,. \tag{15}$$

where GBR_i is the declared target rate of user i, while $i_{ca}(k,\ell)$ accounts for the "goodness" of the RBG when allocated to the ith user and it is computed as[3]

$$i_{ca,PF}(k,\ell) = \frac{r_i(k,\ell)}{\zeta_i(k)}\,. \tag{16}$$

Tab. II summarizes the characteristics of the different schedulers considered in this work.

V. Simulation Setup

To assess the performance of the schedulers in different environments, the Network Simulator version 3.20 (*ns*-3) has been used, which is, at the time of writing, the latest release.

A default EUTRA-Absolute Radio Frequency Channel Number (EARFCN) of 500 is used, that corresponds to a carrier frequency of $f_c = 2.16$ GHz. We use the unacknowledged mode for the radio link control (RLC) layer and the AMC model proposed in [25] for *ns*-3. Various system parameters are summarized in Tab. III while the remaining parameters have been set as for *ns*-3 default setting.

The wireless link is modelled as a path loss plus fading channel. The *ns*-3 LTE module includes a trace-based fading model that makes use of pre-calculated traces to limit the computational complexity of the simulations [6]. All users share the same fading trace but with random starting point in order to have almost independent fading processes. We analyze the behaviour of different scheduling policies both for the flat fading and frequency selective channels, where the traces can be obtained by using the MATLAB script that comes with the *ns*-3 release. We assume that the channel temporal correlation follows Jakes' model, and we denote with ν_d the Doppler spread. Note that, the Doppler effect that determines the time variability of the channel fading usually results from the mobility of the terminals. However, it can also be observed between static devices, when even small variations of the surrounding environment (e.g., due to the

[3]Note that [4] defines two different versions of $i_{ca}(k,\ell)$. Please, refer to the original paper for further details.

TABLE II
MAIN CHARACTERISTICS OF DIFFERENT SCHEDULERS.

Scheduler	MTS	BETS	PFS	FTGS	PSS	CQA
Goal	Maximize spectral efficiency	Maximize fairness	Trade-off between fairness and throughput	Maximize long term throughput and fairness	Maximize throughput with fairness control	Maximize spectral efficiency with latency control
Resource allocation	TD or FD	TD or FD	TD or FD	TD or FD	Hybrid	Hybrid
Required input	RBs current capacity	Average users' throughput	RBs current capacity & average users' throughput	RBs current capacity & average channel-dependent weighting factors	RBs current capacity & average users' throughput	RBs current capacity & average users' throughput & head-of-line packet delays

TABLE III
SYSTEM PARAMETERS SETTING.

Parameter	Value
Number of RBs	25
Bandwidth	5 MHz
RBG size	2
Downlink EARFCN	500
AMC Model	PiroEW2010 [23]
Pathloss model	Friis [24]
Fading model	Trace based
Error mode control	Deactivated
Radio Link Control Mode	Unacknowledged
Tx power of eNode	30 dBm
Tx power of UEs	23 dBm
Noise figure at eNode and UEs	5 dB
Transmission Time Interval	1 ms
TCP packet size	1024 B

TABLE IV
PARAMETERS FOR THE FREQUENCY SELECTIVE CHANNELS.

Pedestrian $\tau_{\mathrm{rms}} = 44$ ns		Vehicular $\tau_{\mathrm{rms}} = 256$ ns		Urban $\tau_{\mathrm{rms}} = 990$ ns	
τ_i (ns)	$E[\lvert g_i^2 \rvert]$ (dB)	τ_i (ns)	$E[\lvert g_i^2 \rvert]$ (dB)	τ_i (ns)	$E[\lvert g_i^2 \rvert]$ (dB)
0	0.0	0	0.0	0	-1.0
30	-1.0	30	-1.5	50	-1.0
70	-2.0	150	-1.4	120	-1.0
90	-3.0	310	-3.6	200	0.0
120	-8.0	370	-0.6	230	0.0
190	-17.2	710	-9.1	500	0.0
410	-20.8	1090	-7.0	1600	-3.0
		1730	-12.0	2300	-5.0
		2510	-16.9	5000	-7.0

the motion of people/vehicles in the transmission zone, the trembling of plants or tree leaves due to the wind, and so on) change the propagation paths of the wireless signal. The temporal variability of the fading between static terminals, therefore, strongly depends on the propagation environment. However, for the sake of generality and replicability, we here consider some reference models that are usually associated with scenarios that involve different degrees of mobility of the transmitter and/or receiver. More specifically, we consider the power delay profiles reported in Tab. IV, which refer to pedestrian, vehicular, and urban environments, with τ_{rms} being 44 ns, 356 ns, and 990 ns, respectively. Frequency selective Rayleigh channels have been generated as proposed by the 3GPP [26].

Unless otherwise specified, simulations are carried out by considering $N = 10$ static UEs, with average SINR values $\{\bar{\gamma}_i\}$ as reported in the first column of Tab. V (the values in the other columns will be described later). The distance of each UE from the base station is determined by reverting the path-loss model, in such a way that each UE experiences the desired average SINR. The linear mean of such values is here referred to as *mean cell SINR*, which is given by

$$\mu_{dB} = 10 \log_{10} \left(\frac{1}{N} \sum_{i=1}^{N} \bar{\gamma}_i \right). \tag{17}$$

It may be worth remarking that μ_{dB} depends on the position of the UEs with respect to the center of the cell, and it will be used in the following to compare scenarios with different UEs' location. For the values in Tab. V, the mean cell SINR turns out to be $\mu_{dB} = 15$ dB.

Simulations have been carried out by considering both saturated UDP traffic sources (that is, saturated traffic at the MAC layer) and saturated TCP sources, which generate traffic toward each UE. While non-saturated traffic models are more realistic, their implementation differ widely making comparison of results from different studies difficult. The saturated (full buffer) traffic model implementations are usually the same and the model is included in almost all studies. Hence, we will base our scheduler performance comparisons on the full buffer traffic model. Each simulation lasts for 60 seconds of simulated time, enough to average out the fading fluctuations and achieving an excellent statistical confidence.[4]

VI. NUMERICAL RESULTS

In this section we present the simulation results for the considered schedulers, under different fading conditions. We initially consider a flat fading channel, and we present results for TD schedulers only. Successively, we consider different frequency selective channels, and simulate both the TD and FD versions of the schedulers.

[4]Since the 95% confidence interval is generally very narrow, it has been omitted from the figures to reduce clutter.

TABLE V
AVERAGE SINR AND FTGS PARAMETERS OF USERS.

i	$\bar{\gamma}_{i,dB}$	α_i	$p(i)$	$\bar{R}_i/W$
1	10.0000	2.9899	0.1490	2.5114
2	11.7041	3.7867	0.1235	3.0292
3	12.9248	4.3845	0.1099	3.4031
4	13.8766	4.8634	0.1012	3.6950
5	14.6568	5.2634	0.0951	3.9342
6	15.3180	5.6070	0.0904	4.1365
7	15.8917	5.9083	0.0868	4.3117
8	16.3984	6.1768	0.0838	4.4662
9	16.8521	6.4190	0.0812	4.6043
10	17.2628	6.6397	0.0791	4.7291

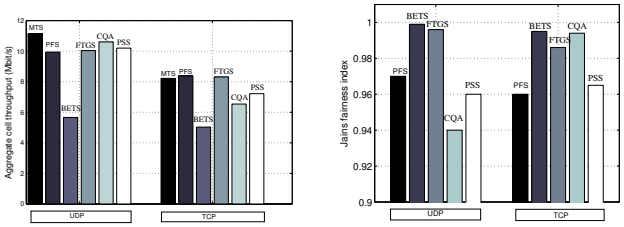

Fig. 4. Average cell rate (left) and Jain's fairness (right) achieved by the schedulers (TD version, when applicable), using a flat fast ($\nu_d = 120$ Hz) fading channel.

A. Flat fading channel

To begin with, we analyze the values in the three rightmost columns of Tab. V, which refer to the parameters used by the FTGS scheduler for each user i, namely the weighting factor α_i, the scheduling probability $p(i)$, and the long-term average rate $\bar{R}_i$ experienced by the user when it gets scheduled. We see that, as expected, the access probability $p(i)$ is lower for users with better channel conditions (i.e., larger $\bar{\gamma}_i$), which are then scheduled more rarely in order to leave more resources to users with poor channel conditions. In this way, the average spectral efficiency of the ith UE, which is equal to

$$\bar{\eta} = \frac{p(i) \cdot \bar{R}_i}{W} = 0.374\,, \tag{18}$$

turns out to be the same for all users, according to the equal throughput guarantee principle embodied by the FTGS algorithm. At the same time, FTGS shall be able to increase the cell efficiency by opportunistically exploiting the channel variations in the short term.

To investigate these properties, we report in Fig. 4 the throughput and the fairness achieved by the different schedulers,[5] both for UDP and TCP saturated traffic, considering a flat fast-fading channel with Doppler spread $\nu_d = 120$ Hz. We can see that, as expected, the opportunistic nature of MTS yields high aggregate cell throughput, both for UDP and TCP traffic sources. Conversely, the channel-agnostic approach of BETS yields the highest fairness in both scenarios, but the overall cell throughput is considerably reduced. FTGS, PFS, CQA and PSS, instead, perform fairly well both in terms of throughput and fairness, though the fairness performance is slightly more erratic among the schedulers.

[5]Note that, to better appreciate the comparison between the fairness performance of the other algorithms, we removed the fairness results for MTS, whose Jain's fairness index is significantly lower than that of the other algorithms, being approximately equal to 0.62 and 0.82 for the UDP and TCP cases, respectively.

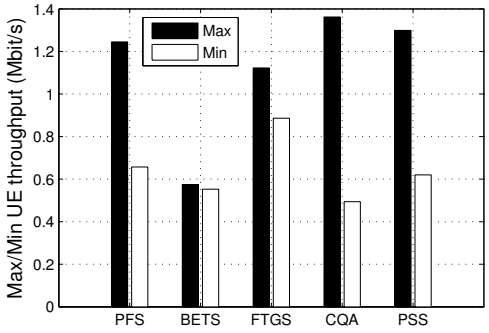

Fig. 5. Minimum and Maximum average throughput per UE achieved by the considered schedulers, using a flat fast ($\nu_d = 120$ Hz) fading channel and an UDP saturated traffic.

To gain more insight on the performance of the schedulers, we focus on saturated UDP sources, which make it possible to analyze the performance of the different schedulers in terms of MAC-layer throughput and inter-scheduling delay statistics without the traffic fluctuations generated by the TCP congestion control mechanisms. We hence report in Fig. 5 the best and worse user average throughput for the different schedulers (with the exception of MTS that is not concerned with users' fairness). We observe that, using PFS and PSS, the best user gets approximately twice the average rate of the worst user, with a clear penalization of the UEs with worse channel conditions. CQA penalizes the worst user even more. This gap, using FTGS, reduces to 21%, showing that FTGS is able to provide similar throughput to all the users in the system, irrespective of their $\bar{\gamma}$. BETS achieves the best performance balance among the users, but at the cost of a low spectrum efficiency of the cell.

Another aspect of interest is the inter-scheduling time of a UE at MAC layer, which is defined here as the time interval between two consecutive scheduling instants of the UE. In [12], authors have shown that the inter-scheduling time at the MAC layer can have adverse effects on the TCP congestion control mechanism. Furthermore, inter-scheduling time is related to the delay experienced by users that try to access the channel, and can have a strong impact on applications where delay plays a major role in determining the quality of experience of the final user.

Since FTGS scheduling decision depends on the channel variations, we argue that in case of slow fading, the inter-scheduling time could be considerably long. The TD approach exhibits higher inter-scheduling time, because all resources in the same TTI are allocated to the same user. In FD approach, instead, RBGs in the same TTI can be allocated to different users, leading, on average, to shorter inter-scheduling time, but also smaller transmit capacity at each scheduling event. It is therefore of interest to evaluate the inter-scheduling time in different channel conditions.

TABLE VI
PROBABILITY OF $\delta = 1$ TTI FOR SLOW ($\nu_d = 6$ HZ) AND FAST ($\nu_d = 120$ HZ) FADING CHANNELS.

	BETS	PFS	FTGS	CQA	PSS
Slow fading	0.017	0.20	0.95	0.95	0.28
Fast fading	0.011	0.37	0.49	0.50	0.44

The inter-scheduling time has been analyzed assuming the TD approach, and considering a fast ($\nu_d = 120$ Hz) and a slow ($\nu_d = 6$ Hz) fading environment. We carry out a worst-case analysis by considering the inter-scheduling time of the UE which is scheduled less frequently. Once again, we omit MTS from this comparison since, with this algorithm, the inter-scheduling time of the worst user is much larger than that given by the other schedulers.

Let δ denote the random variable that models the (worst-case) inter-scheduling time for a certain scheduler. From the simulation results, we observed that the empirical statistical distribution of δ exhibits a peak at the TTI duration, i.e., 1 ms, meaning that the scheduling of each UE occurs in a bursty manner, with runs of subframes assigned to a single UE, followed by periods during which other UEs are served.

In particular Tab. VI shows the probability that $\delta = 1$ ms for the different schedulers under a slow ($\nu_d = 6$ Hz) and fast ($\nu_d = 120$ Hz) fading environment. The probability is significant for FTGS and CQA in both the environments, which indicates the attitude of these algorithms to allocate resources in a very bursty manner. For BETS the fading environment is not very relevant, and the considered probability is small enough to relate BETS to Round Robin Polling, which always assigns resources to different users in consecutive time intervals. Finally PFS and PSS lie in the middle.

To appreciate the impact of the fading on the different schedulers, it is interesting to investigate the tail of the distribution of δ. To this end, we report in Fig. 6 the *conditional* empirical cumulative distribution function (ECDF) of δ, given that $\delta > 1$ ms. This conditional ECDF captures the statistical distribution of the time in-between consecutive runs of subframes allocated to the same UE, which is a lower bound of the packet service time at the data link layer (DLL).

In Fig. 6 we plot results both in the case of slow (solid-lines with full markers) and fast (dashed-lines with empty markers) flat fading channels. We see that the conditional statistical distribution of the inter-scheduling time of BETS is not strongly influenced by the dynamics of the fading process, as expected given the channel-agnostic scheduling policy applied by the algorithm. PFS and PSS inter-scheduling times exhibit a more pronounced dependence on the fading process, because the scheduling policies also consider the current UEs' channel state. Nonetheless, in most of the cases, δ does not exceed 110 ms. The UEs scheduling order imposed by FTGS and CQA, instead, is more sensitive to channel variations, so that the tail distribution of the inter-scheduling time of these schedulers changes quite significantly for fast and slow channels. We can indeed observe that, while with fast fading the FTGS and CQA maximum δ is comparable

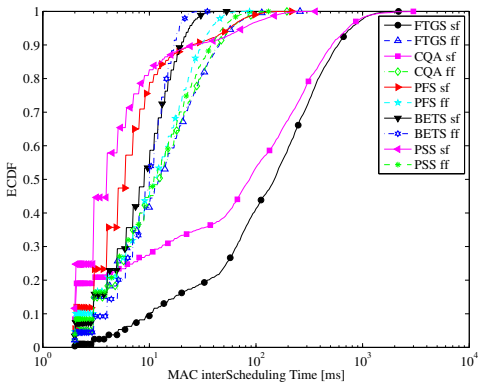

Fig. 6. Conditional ECDF of the inter-scheduling time δ, given that $\delta > 1$ ms, for the TD version of FTGS, CQA, PFS, BETS and PSS. Solid lines: *slow* flat (sf) fading channels ($\nu_d = 6$ Hz); dashed lines: *fast* flat (ff) fading channel ($\nu_d = 120$ Hz).

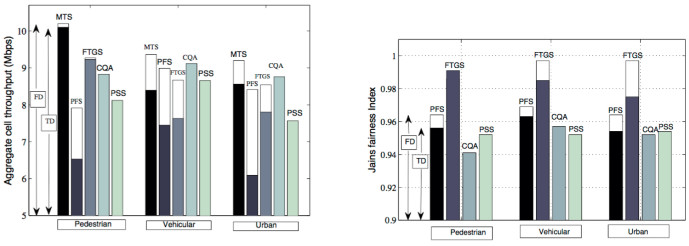

Fig. 7. Aggregate cell throughput (left) and Jain's fairness index (right) for the FD and TD versions of MTS, PFS and FTGS, and for CQA and PSS, with three different frequency selective channels, using UDP sources. Colored bar shows the rate using the TD version, while white bar on top quantifies the improvement brought by the FD version. CQA and PSS, being joint TD/FD schedulers, are represented by a single solid bar.

with that of the other algorithms, with slow fading there is a non negligible probability that δ exceeds 1 s. In this case, the packet service time at the MAC layer can sporadically become very large, making this scheduler unsuitable for real time applications. Finally, in slow fading channels, CQA tends to have shorter inter-scheduling times than FTGS. As we will see in the next section, however, the FD version of the FTGS can dramatically improve this performance index in frequency selective channels.

B. Frequency selective channel

We now turn our attention to frequency selective channels, for which we compare the performance of TD and FD versions of the schedulers to determine whether the increased computational complexity of FD is paid back in terms of significant performance gain or not.

Fig. 7 shows the aggregate cell throughput and the Jain's fairness index achieved by the FD and TD versions of MTS, PFS, and FTGS, and by CQA and PSS, with saturated UDP sources, for the three channel models (Pedestrian, Vehicular and Urban) described in detail earlier in Sec. V. Note that MTS's fairness results are omitted being significantly lower than the others. CQA and PSS, being joint FD and TD scheduler, are only shown by a single solid bar. BETS performance will be discussed later, due to its peculiar nature.

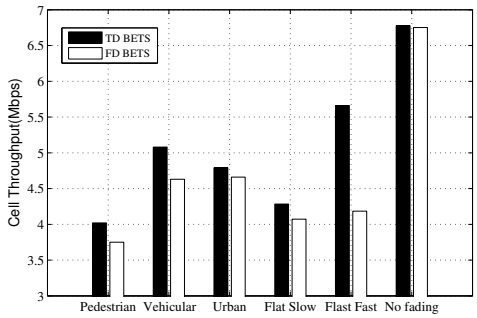

Fig. 8. Cell Throughput for FD and TD BETS with UDP sources.

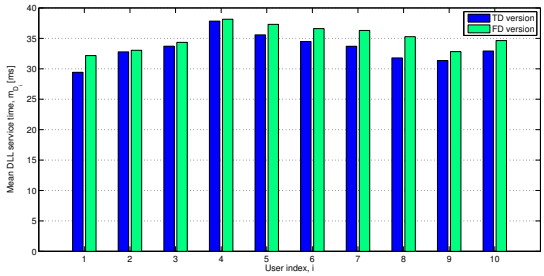

Fig. 9. Mean DLL service time m_{D_i} for the TD and FD approach, over a time dispersive channel with Doppler spread $\nu_d = 120$ Hz.

Comparing Fig. 7 with Fig. 4, we observe a general throughput loss with respect to the flat fading case, which is only partially compensated by the introduction of the FD version of the algorithms. Furthermore, we note that the performance gap between the FD and TD versions of each scheduler generally widens for scenarios with higher channel dispersion.

As expected, the MTS achieves the highest throughput, at the cost of a very low fairness (not reported in the paper). Moreover, we note that, consistently with [27], PFS performs better when the channel is more dispersive, in particular in the FD version. PFS throughput can in fact be expressed as the sum of two terms: the first models the throughput achieved using a Round Robin Scheduler (RRS), while the second is the improvement brought in by the opportunistic approach used by PFS, which is positively correlated to the channel dispersion. PFS, therefore, performs better in severe fading environments. On the other hand, the opportunistic based scheduling policies (such as MTS and FTGS) achieve higher throughput in almost-flat channel environments, where τ_{rms} is smaller.

An important observation with regard to average cell throughput is that CQA overtakes FTGS for both vehicular and urban scenarios, though PSS performs the worst in urban environment. The small loss in terms of cell throughput of FTGS with respect to the hybrid schedulers is however balanced by a better fairness, as shown in the right-hand side graph of Fig. 7. In fact, we see that both the TD and FD versions of FTGS outperforms all other schedulers in terms of fairness for all the three considered scenarios. Also the TD and FD version of FTGS gives the same fairness in pedestrian environment.

The aggregate cell throughput achieved by the TD and FD versions of BETS, shown in Fig. 8, deserves a separate discussion. As a first thing, we observe that, conversely to the other considered schedulers, the FD version of BETS achieves lower aggregate cell throughput than the TD version in all scenarios, except that with no fading, where the two versions perform similarly. Second, the FD-BETS performance is worse in presence of flat-fading channels, or slowly-varying frequency selective fading (pedestrian scenario). Therefore, when all the RBGs in a subframe are approximately equivalent for a certain user, the possibility of scheduling different users in the same subframe seems to yield a lower aggregate cell throughput. This result is apparently counterintuitive, since a larger flexibility in resource allocation is expected to bring higher performance. An intuitive explanation for such an apparent contradiction is the following. Suppose UE i has the lowest average throughput when subframe k starts. TD-BETS will hence assign all the RBGs in the subframe to user i, irrespective of the actual value of $r_i(k)$. Conversely, FD-BETS will assign only the RBGs needed to compensate the throughput gap of UE i with respect to the other UEs. Therefore, if the channel is particularly good, i.e., $r_i(k,\ell)$ is large, it is likely that just a few RBGs will be allocated to user i, while the remaining RBGs will instead be allocated to other users. In this way, the fairness is maximized, but at the cost of a lower utilization of good channel conditions and, hence, a lower average cell throughput. Unfortunately, the gain in terms of fairness turns out to be almost negligible, since the TD version already achieves excellent results, while the reduction in cell throughput is relevant, as can be observed from Fig. 8.

We now turn our attention back to inter-scheduling time for the FTGS. While it is easily predictable that the possibility of scheduling multiple UEs in the same time slot will generally reduce δ, and compact its ECDF, the effect of FD on the data link layer (DLL) packet service time is less obvious, because the increased scheduling frequency of each UE comes together with a more fractioned amount of allocated resources. To shed some light on these aspects, we introduce the DLL service time D_i, which is defined as the time that the i-th UE takes to complete the transmission of the head-of-line DLL packet.

In Appendix A-II we derive approximate expressions of the mean m_{D_i} and standard deviation σ_{D_i} of D_i as functions of the empirical distribution of the inter-scheduling time δ and of the amount of bits sent at each scheduling event. Fig. 9 and Fig. 10 report m_{D_i} and σ_{D_i}, respectively, for each user i, in a vehicular scenario, assuming DLL packets of $L = 4096$ bytes. Since FTGS guarantees the same long term throughput to all users, both the TD and FD versions of the scheduler yield approximately the same m_{D_i} for each i, irrespective of $\bar{\gamma}_i$. However, we note that the FD version of FTGS dramatically decreases σ_{D_i}, thus offering a more predictable service time to the upper layers. As a side note, we observe that σ_{D_i} is slightly higher for users with better average channel conditions (i.e., larger $\bar{\gamma}_i$), which are indeed scheduled more rarely.

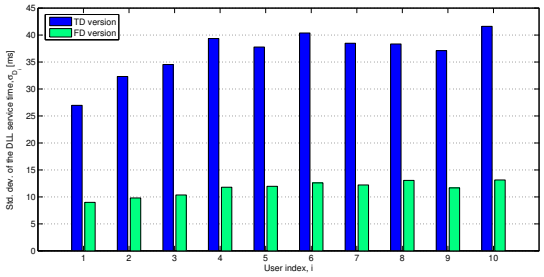

Fig. 10. σ_{D_i} for the TD and FD approach, over a time dispersive channel with Doppler spread $\nu_d = 120$ Hz.

C. Analysis of the opportunistic gain of FTGS

The performance analysis carried out so far shows that FTGS is capable of providing high fairness among the UEs, while opportunistically exploiting channel variations to increase the cell throughput. In this section we attempt to quantify such an opportunistic gain when the users average SINRs are more disparate. As benchmark, we consider the performance of TD-BETS, which guarantees equal long-term throughput to all users, but without considering the *current* rates of the different RBGs in the scheduling policy. The analytical expressions of TD-BETS cell throughput and spectral efficiency are derived in Appendix A-III.

We hence define the *opportunistic gain* as

$$\phi = \frac{\eta_{FTGS}}{\eta_{BETS}} - 1. \tag{19}$$

where η_{FTGS} is the cell spectral efficiency achieved by FTGS, while η_{BETS} is the cell spectral efficiency of BETS. In Appendix, we derive an analytical expression for η_{BETS}, which can hence be computed mathematically using (A-22). Unfortunately, we have not been able to find a mathematical expression for η_{FTGS}, which has hence been estimated via simulation.

In all previous results, UEs were located in the LTE cell in order to experience average SINRs in the interval $[10\ dB, 17.26\ dB]$, as reported in Tab. V, with mean cell SINR $\mu_{dB} = 15$ dB. We now investigate the FTGS performance when varying the span Δ of SINRs interval. More precisely, we fix the maximum SINR to $\bar{\gamma}_{max} = 25$ dB and progressively decrease the minimum SINR, thus enlarging Δ and varying the mean cell SINR, μ_{dB}. Note that the SINRs are equally spaced in *linear scale*, thus resulting in a logarithmic distribution over the interval in dB scale.

In Fig. 11 we report the opportunistic gain ϕ when varying μ_{dB}, and for an increasing number N of UEs in the cell. From the figure, it is apparent that the opportunistic gain of FTGS is larger when users average SINRs are more disparate, since in this condition a channel-aware policy can partially compensate for the worse channel conditions of the more unlucky users. Furthermore, the opportunistic gain increases when the population of users in a given SINR range grows, thus making the opportunistic policies particularly interesting when the number of users is large [28].

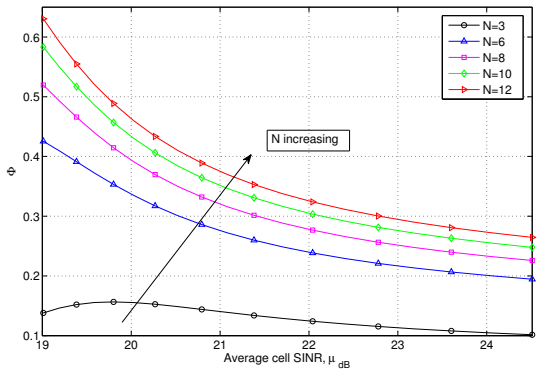

Fig. 11. Cell spectral efficiency gain of FTGS over BETS (TD versions) when varying μ_{dB}, with $\bar{\gamma}_{max} = 25$ dB.

D. Robustness of FTGS to imperfect channel estimation

Throughout this work we have assumed that the eNodeB computes the FTGS parameters under the assumption that the different signals are affected by Rayleigh fading. To evaluate the robustness of FTGS, we evaluate the performance loss incurred by FTGS when the different signals are affected by Rician fading.

We hence generated two new fading traces, named Rice1 and Rice2, using the vehicular power delay profile described in Tab. IV, but adding a strong line-of-sight (LOS) component in the first path for Rice1, and in the first, second and third paths for Rice2. The remaining paths were still assumed to be affected by Rayleigh fading. The Rice factors of the paths affected by Rician fading were set to $K_1 = 20$ dB in Rice1, and $K_1 = 10$ dB, $K_2 = K_3 = 0$ dB in Rice2.

Fig. 12 shows the cell aggregate throughput and the Jain's fairness index for the three channel models, namely Rayleigh, Rice1 and Rice2. We can see that the performance loss of FTGS in presence of strong LOS components in the received signals is insignificant in terms of fairness, and quite limited for the throughput, so that we can conclude that the scheduler is rather robust to different fading models and to small errors in the estimate of the system parameters. We observe that the FTGS algorithm can be adjusted to other fading distributions but, in this case, the eNodeB should be able to estimate the most suitable statistical model for the channel from the CQI values returned by the UEs, which is an error-prone and time/resource consuming process. In fact, considering the mapping provided in Tab. I, the CQI values span an SNR interval of about 25 dB with uneven step. Therefore, the estimate of the channel gain from CQI values is quite rough and noisy. On the other hand, considering the robustness exhibited by FTGS to errors and non idealities in the channel model, increasing the number of levels of the CQI to enhance the accuracy of the SNR estimate is not expected to bring any significant performance gain.

VII. Conclusions and Future Work

In this work, we carried out a performance analysis of different LTE downlink schedulers, namely MTS, BETS, PFS, FTGS, CQA and PSS, in presence of flat and frequency

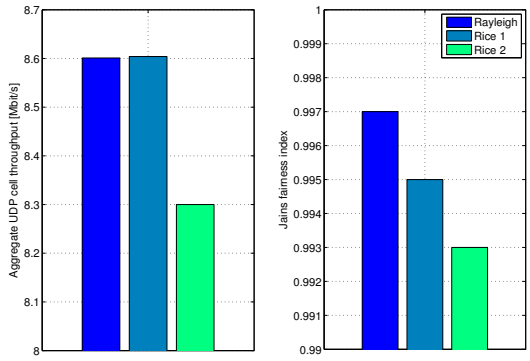

Fig. 12. Cell throughput and Jain fairness index in case of Rayleigh and Rice channels.

selective fading channels, and both for saturated UDP and TCP traffic source models. Besides the standard time-domain (TD) scheduling mode, where all RBs in a subframe can be allocated to a single UE, we also considered their frequency-domain (FD) mode, where the RBs in each subframe can allotted to multiple UEs, in an exclusive manner. The scheduling indexes of the schedulers have been changed accordingly, to account for the finer granularity in resource allocation and the richer CQI returned by each UE. Furthermore, both the TD and FD versions of FTGS have been implemented in *ns*-3, thus enriching the simulation platform with a scheduler that provides throughput guarantees to the UEs.

The simulation comparison has revealed that FTGS is indeed able to improve the cell spectral efficiency with respect to BETS and PFS, achieving similar performance as CQA and PSS, but with better users' fairness, almost comparable with that of BETS. Furthermore, the FD version of FTGS yields a significant performance improvement over the TD version, both in terms of throughput and users' fairness, for dispersive frequency-selective channels. The impact of the scheduling algorithms on the delay sensitive applications is also studied by analyzing the inter-scheduling time. It is observed that the FD version of the FTGS can substantially reduce the inter-scheduling time as compared to the TD version. In conclusion, it is shown that FTGS, which assumes to know the statistical distribution of users' SINR, is capable of increasing the throughput fairness among users without affecting much the cell efficiency.

In practical scenarios, however, the knowledge of the SINR statistical distribution may actually be difficult to obtain. Although we have shown that FTGS is rather robust to wrong estimation of the SINR distribution, the design of schedulers that perform a dynamic estimate of the SINR distribution from the CQI feedback and adapt accordingly remains an interesting subject for future studies. Furthermore, the current version of FTGS has been designed to provide (almost) equal long-term throughput to all users, irrespective of their average channel conditions. This characteristic, however, may yield quite low spectral efficiency in case of users with low average SINR, e.g., at the edge of the cell. Therefore, a matter for future work is the design of schedulers that differentiate the throughput guarantees according to the average channel quality of the users, in order to provide sufficient quality of experience to edge users, while limiting their impact on the performance of the other users. Finally, extending the study to more sophisticated scenarios, which account for terminals mobility, common traffic patterns, urban/suburban landscapes, and so on, can provide new insights and ideas to design more effective scheduling algorithms in realistic settings.

APPENDIX

A-I. Derivation of FTGS coefficients

For self-consistency of the paper, we here recall (and slightly revise) the mathematical argumentation developed in [7] to determine the coefficients of the TD version of FTGS.

The aim of the TD version of FTGS is to provide the same long-term throughput to all UEs, while exploiting the channel variability to increase the aggregate cell throughput. Then, considering an arbitrarily long time interval T_W, the amount of bits that each UE shall be able to receive can be expressed as

$$B = T_i \bar{R}_i, \tag{A-1}$$

where T_i is the time allocated to user i in the time window T_W, and $\bar{R}_i$ is the average rate experienced by user i when it is scheduled. Furthermore, assuming that the system is *work conserving*, we require

$$\sum_{i=1}^{N} T_i = T_W \,. \tag{A-2}$$

Denoting by $p(i)$ the access probability of the i-th UE, i.e., the fraction of the time user i is scheduled within the time window, (A-1) can also be expressed as

$$B = p(i) T_W \bar{R}_i \,. \tag{A-3}$$

The objective is then to find the scheduling probabilities $\{p(i)\}$ for which B is maximized. We observe that, by combining (A-1)-(A-3), we get

$$p(i) = \frac{1}{\bar{R}_i \sum_{j=1}^{N} \bar{R}_j{}^{-1}} \,, \tag{A-4}$$

so that we need first to find a proper expression for $\bar{R}_i$.

The average rate experienced by user i when scheduled can then be expressed as follows,

$$\bar{R}_i = W \int_0^{\infty} \log_2 \left(1 + \frac{\gamma}{\Gamma}\right) p_\gamma(\gamma|i) d\gamma, \tag{A-5}$$

where $p_\gamma(\gamma|i)$ is the probability density function (PDF) of the SINR given that user i is scheduled, and W is the available bandwidth. Assuming a Rayleigh fading channel, and denoting by $\bar{\gamma}_i$ the average SINR for user i, the cumulative distribution function (CDF) of the channel SINR is given by

$$P_{\gamma_i}(x) = P[\gamma_i \le x] = 1 - e^{-x/\bar{\gamma}_i}. \tag{A-6}$$

We now define a new random variable (r.v.) $S_i \triangleq R_i/\alpha_i$ where R_i is the r.v. that describes the instantaneous rate of user i. Therefore, S_i models the priority metric used by the

algorithm, as for (7). The value of S_i with SINR γ is given by

$$S_i(\gamma) = \frac{W \log_2\left(1+\frac{\gamma}{\Gamma}\right)}{\alpha_i}. \quad \text{(A-7)}$$

The CDF of S_i using (A-6) is given by

$$P_{S_i}(s) = P[S_i(\gamma) < s] = 1 - e^{c/\bar{\gamma}_i}, \quad \text{(A-8)}$$

where $c = \Gamma \cdot \left(1 - 2^{\frac{\alpha_i s}{W}}\right)$. The corresponding PDF is then equal to

$$p_{S_i}(s) = \frac{\ln(2)\alpha_i}{W\bar{\gamma}_i}(\Gamma - c)e^{c/\bar{\gamma}_i}. \quad \text{(A-9)}$$

Since S_i is the scheduling metric of FTGS, we can express the access probability of user i as

$$p(i) = P\Big[S_i > \max_{j\neq i} S_j\Big] = \int_0^\infty p_{S_i}(s) \prod_{j=1, j\neq i}^{N} P_{S_j}(s)\mathrm{d}s. \quad \text{(A-10)}$$

Now, using Bayes' rule, we get the PDF of S_i given that user i is scheduled as

$$p_{S_i}(s|i) = \frac{p_{S_i}(s)}{p(i)} \prod_{j=1, j\neq i}^{N} P_{S_j}(s). \quad \text{(A-11)}$$

The conditional expectation of S_i given i is then equal to

$$\bar{R}_i = \alpha_i \int_0^\infty s \cdot p_{S_i}(s|i) ds, \quad \text{(A-12)}$$

from which we obtain

$$p(i) = \frac{\alpha_i}{\bar{R}_i} \int_0^\infty s \cdot p_{S_i}(s) \prod_{j=1, j\neq i}^{N} P_{S_j}(s)\mathrm{d}s. \quad \text{(A-13)}$$

By combining (A-4), (A-10), and (A-13) we finally get a set of $3N$ independent equations in $3N$ unknowns, namely $\{\alpha_i, \bar{R}_i, p(i)\}$, $i = 1, 2, ..., N$, which can be solved using standard numerical tools [7] (e.g., those implemented in the `fsolve` function of MATLAB). However, the regular shape of the involved functions makes it possible to speed up the computation of the unknowns, provided that the solving algorithm is started from a point that is relatively close to the solution. A good starting point is obtained by setting $\bar{R}_i^{(1)} = \mathrm{E}[R_i]$ and $p(i)^{(1)} = \left(\bar{R}_i^{(1)} / \prod_j \bar{R}_j^{(1)}\right)^{-1}$, as for (A-4), and $\alpha_i^{(1)} = \bar{R}_i^{(1)}$. However, the application of FTGS in a dynamic scenario will require the development of faster algorithms to estimate the coefficients α_i.

A-II. DLL PACKET SERVICE TIME STATISTICS

We here derive approximate expressions for the first and second order moments of the data link layer (DLL) service time D for a packet of L bits, as functions of the empirical first, second and third order statistical moment of the inter-scheduling time δ_k, and of the number of bits b_k transmitted by the tagged UE at the kth scheduling event. Note that, the symbols m_x, σ_x^2, and $M_x^{(3)}$ will be used to denote the statistical mean, the variance, and the third-order moment of a generic random variable x, respectively.

Let Y_ℓ be the number of subframes required to transmit (at least) $\ell \geq 1$ bits. The service time D for a packet of L bits can then be expressed as $D = \sum_{k=1}^{Y_L} \delta_k$ from which we get

$$m_D = m_{Y_L} m_\delta\,, \quad \text{and} \quad \sigma_D^2 = m_{Y_L}\sigma_\delta^2 + \sigma_{Y_L}^2 m_\delta^2\,. \quad \text{(A-14)}$$

We hence need to express m_{Y_L} and $\sigma_{Y_L}^2$ in terms of the statistical moments of the random variables b_k. To this end, we introduce $S_n = \sum_{k=1}^{n} b_k$, which is the random variable that denotes the total number of bits sent by a UE after n scheduling events. We hence have

$$S_{Y_L} = \sum_{k=1}^{Y_L} b_k = L + \tilde{b}\,, \quad \text{(A-15)}$$

where $\tilde{b}$ is the number of bits allocated in excess of the actual packet size in the last scheduling event. For simplicity, we assume $\{b_k\}$ are independent and identically distributed random variables. From (A-15), using results for random sum of random variables [29], the mean and variance of S_{Y_L} can be expressed as

$$m_{S_{Y_L}} = m_{Y_L} m_b = L + m_{\tilde{b}}\,, \quad \text{and} \quad \sigma_{S_{Y_L}}^2 = m_{Y_L}\sigma_b^2 + \sigma_{Y_L}^2 m_b^2 = \sigma_{\tilde{b}}^2\,, \quad \text{(A-16)}$$

from which

$$m_{Y_L} = (L + m_{\tilde{b}})/m_b\,, \quad \text{and} \quad \sigma_{Y_L}^2 = (\sigma_{\tilde{b}}^2 - m_{Y_L}\sigma_b^2)/m_b^2\,. \quad \text{(A-17)}$$

It remains to determine the expression of $m_{\tilde{b}}$ and $\sigma_{\tilde{b}}^2$. We then observe that $\tilde{b}$ can be seen as the *forward excess process* of a renewal process with renewal times, $\{Y_\ell, \ell \geq 1\}$. Therefore, for sufficiently large L, the mean and variance of $\tilde{b}$ can be approximated with their asymptotic values that, according to the *inspection paradox*, are given by $m_{\tilde{b}} = (m_b^2 + \sigma_b^2)/(2m_b)$, and $\sigma_{\tilde{b}}^2 = M_b^{(3)}/(3m_b)$, which concludes the derivation.

A-III. LONG-TERM THROUGHPUT OF BETS

We consider N users with average SINR $\{\bar{\gamma}_i\}$, $i = 1, 2, ..., N$. Furthermore, we assume that the received signals are affected by independent Rayleigh fading processes, so that the SINR experienced by user i on any RBG can be expressed as $\gamma_i = \varepsilon_i\bar{\gamma}_i$, where ε_i is an exponentially distributed random variable of unit mean. Let the average rate experience by user i any time it gets scheduled be denoted by $\bar{G}_i$. Since the resource allocation criterion of BETS does not account for γ_i, $\bar{G}_i$ can be expressed as

$$\bar{G}_i = \mathcal{B}\,\mathbf{E}\left[\log_2\left(1+\frac{\varepsilon_i\bar{\gamma}_i}{\Gamma}\right)\right] = \mathcal{B}\log_2(e)e^{\frac{\Gamma}{\bar{\gamma}_i}}\,E_i\left(\frac{\Gamma}{\bar{\gamma}_i}\right) \quad \text{(A-18)}$$

where $\mathcal{B}$ is the bandwidth of each RBG and $E_i(x) = \int_x^\infty (e^{-t}/t)\mathrm{d}t$ is the exponential integral function.

For ease of explanation, we consider the TD version of the scheduler, though the reasoning can be straightforwardly extended to the FD versions. Since BETS is designed to ideally provide long-term fairness, in a sufficiently long time interval T, all users will transmit an equal amount of bits B. Hence,

the total time allotted to user i in the time window T will be equal to $T_i = B/\bar{G}_i$ for all $i \in \{1, \ldots, N\}$. Therefore, we get

$$T = \sum_{i=1}^{N} T_i = \sum_{i=1}^{N} \frac{B}{\bar{G}_i}, \tag{A-19}$$

from which we obtain

$$B = \frac{T}{\sum_{i=1}^{N}(1/\bar{G}_i)}. \tag{A-20}$$

Finally, the cell throughput can be computed as

$$S_{BETS} = \frac{N\,B}{T} = \frac{N}{\sum_{i=1}^{N}(1/\bar{G}_i)}, \tag{A-21}$$

and the corresponding cell spectral efficiency as

$$\eta_{BETS} = \frac{S}{\mathcal{B}} = \frac{N \log_2(e)}{\sum_{i=1}^{N} e^{-\frac{\Gamma}{\bar{\gamma}_i}} \left[E_i \left(-\frac{\Gamma}{\bar{\gamma}_i} \right) \right]^{-1}}. \tag{A-22}$$

REFERENCES

[1] Ericsson, "Ericsson Mobility Report," http://www.ericsson.com/res/docs/2014/ericsson-mobility-report-june-2014.pdf/, 2014, [Online; accessed 25-August-2014].

[2] F. Capozzi, G. Piro, L. A. Grieco, G. Boggia, and P. Camarda, "Downlink Packet Scheduling in LTE Cellular Networks: Key Design Issues and a Survey." *IEEE Communications Surveys and Tutorials*, vol. 15, no. 2, pp. 678–700, 2013.

[3] W. K. Wong, H. Y. Tang, and V. C. M. Leung, "Token bank fair queuing: a new scheduling algorithm for wireless multimedia services." *Int. J. Communication Systems*, vol. 17, no. 6, pp. 591–614, 2004.

[4] B. Bojovic and N. Baldo, "A new channel and QoS aware scheduler to enhance the capacity of voice over LTE systems," in *11th International Multi-Conference on Systems, Signals Devices (SSD)*, Feb 2014, pp. 1–6.

[5] G. Monghal, K. Pedersen, I. Kovacs, and P. Mogensen, "QoS Oriented Time and Frequency Domain Packet Schedulers for The UTRAN Long Term Evolution," in *IEEE Vehicular Technology Conference (VTC)*, May 2008, pp. 2532–2536.

[6] "Lena module design documentation for ns3," http://www.nsnam.org/docs/models/html/lte-design.html, July 2014.

[7] J. Rasool, V. Hassel, S. de la Kethulle de Ryhove, and G. E. Øien, "Opportunistic scheduling policies for improved throughput guarantees in wireless networks," *EURASIP J. Wireless Comm. and Networking*, vol. 43, pp. 1–18, 2011.

[8] B. Wang, J. Kurose, P. Shenoy, and D. Towsley, "Multimedia Streaming via TCP: An Analytic Performance Study," *ACM Trans. Multimedia Comput. Commun. Appl.*, vol. 4, no. 2, pp. 16:1–16:22, May 2008.

[9] D. Zhou, N. Baldo, and M. Miozzo, "Implementation and validation of LTE downlink schedulers for ns-3," in *Proceedings of the 6th International Conference on Simulation Tools and Techniques (ICST)*, ser. SimuTools '13, 2013, pp. 211–218.

[10] D. Zhou, W. Song, N. Baldo, and M. Miozzo, "Evaluation of TCP performance with LTE downlink schedulers in a vehicular environment," in *IEEE IWCMC*, 2013, pp. 1064–1069.

[11] N. Shojaedin, M. Ghaderi, and A. Sridharan, "TCP-aware scheduling in LTE network," in *IEEE WowMoM*, 2014.

[12] T. E. Klein, K. K. Leung, and H. Zheng, "Improved TCP performance in wireless IP networks through enhanced opportunistic scheduling algorithms." in *IEEE GLOBECOM*, 2004, pp. 2744–2748.

[13] R. Kwan, C. Leung, and J. Zhang, "Proportional fair multiuser scheduling in LTE," *IEEE Signal Processing Letters*, vol. 16, no. 6, pp. 461–464, June 2009.

[14] J. Niu, D. Lee, X. Ren, G. Li, and T. Su, "Scheduling exploiting frequency and multi-user diversity in LTE downlink systems," in *IEEE International Symposium on Personal Indoor and Mobile Radio Communications (PIMRC)*, Sept 2012, pp. 1412–1417.

[15] A. Biernacki and K. Tutschku, "Comparative performance study of LTE downlink schedulers." *Wireless Personal Communications*, vol. 74, no. 2, pp. 585–599, 2014. [Online]. Available: http://dx.doi.org/10.1007/s11277-013-1308-4

[16] S. Sesia, I. Toufik, and M. Baker, *LTE - The UMTS Long Term Evolution: From Theory to Practice*, 2nd ed. Wiley, Sep. 2011.

[17] H. Seo and B. G. Lee, "A proportional-fair power allocation scheme for fair and efficient multiuser OFDM systems." in *IEEE GLOBECOM*, 2004, pp. 3737–3741.

[18] J. Blumenstein, J. C. Ikuno, J. Prokopec, and M. Rupp, "Simulating the long term evolution uplink physical layer," in *53rd International Symposium ELMAR-2011*, Zadar, Croatia, September 2011.

[19] *3GPP TSG-RAN WG1*, R1-081483 ed., Third generation partnership project, April 2008.

[20] R. K. Jain, D.-M. Chiu, and W. Hawe, "A quantitative measure of fairness and discrimination for resource allocation in shared computer system," *ACM Transaction on Computer Systems*, 1984.

[21] V. Hassel, G. Ø ien, and D. Gesbert, "Throughput guarantees for wireless networks with opportunistic scheduling: a comparative study," *IEEE Transactions on Wireless Communications*, vol. 6, no. 12, pp. 4215–4220, December 2007.

[22] N. Benvenuto and G. Cherubini, *Algorithms for Communications Systems and Their Applications*. Wiley, 2002.

[23] G. Piro, L. A. Grieco, G. Boggia, and P. Camarda, "A two-level scheduling algorithm for qos support in the downlink of lte cellular networks," in *Wireless Conference (EW), 2010 European*, April 2010, pp. 246–253.

[24] J. C. Liberti and T. S. Rappaport, "A geometrically based model for line-of-sight multipath radio channels," in *IEEE Vehicular Technology Conference, 1996. Mobile Technology for the Human Race*, vol. 2. IEEE, 1996, pp. 844–848.

[25] G. Piro, N. Baldo, and M. Miozzo, "An LTE module for the ns-3 network simulator." in *SimuTools*, J. Liu, F. Quaglia, S. Eidenbenz, and S. Gilmore, Eds. ICST/ACM, 2011, pp. 415–422.

[26] *3GPP TS 36.104 version 8.3.0 Release 8*, 8th ed., Third generation partnership project, November 2008.

[27] E. Liu and K. K. Leung, "Fair resource allocation under Rayleigh and/or Rician fading environments." in *IEEE PIMRC*, 2008, pp. 1–5.

[28] R. Knopp and P. Humblet, "Information capacity and power control in single-cell multiuser communications," in *IEEE International Conference on Communications (ICC)*, vol. 1, Jun 1995, pp. 331–335.

[29] S. M. Ross, *Introduction to Probability Models, Eighth Edition*, 8th ed. Academic Press, Jan. 2003.